THE ASTROPHYSICAL JOURNAL, 252:54–68, 1982 January 1


# A HIGH-RESOLUTION SPECTROSCOPIC STUDY OF Q0119−046 AND THE NATURE OF ABSORPTION COMPLEXES WITH $z_{abs} > z_{em}$

WALLACE L. W. SARGENT AND PETER YOUNG
Palomar Observatory, California Institute of Technology
AND
A. BOKSENBERG
Department of Physics and Astronomy, University College London
*Received 1981 April 20; accepted 1981 July 10*

## ABSTRACT

High-resolution (0.8 Å FWHM) spectroscopic observations over the wavelength range from 3260 Å to 4920 Å are presented for the QSO Q0119−046 ($z_{em} = 1.937$). We find 61 absorption lines in this object and identify seven main absorption line redshifts ranging from $z_{abs} = 0.6577$ to 1.9751. Some of these systems exhibit velocity structure on a scale of $\lesssim 200$ km s$^{-1}$. There is a complex of three main systems with $z_{abs} > z_{em}$, with "infall" velocities relative to the QSO ranging from −2780 to −3870 km s$^{-1}$. This complex at $z_{abs} = 1.97$ has highly ionized species of C IV, Si IV, and N V, and the ionization parameter $\Upsilon$ lies in the range from 100 to 300 for the various members of the complex. The strongest absorption system of the complex shows C II $\lambda$1334 and excited fine structure C II* $\lambda$1335 lines, and demands a gas density $n(\mathrm{H}) > 100$ cm$^{-3}$.

We discuss the nature of the $z_{abs} > z_{em}$ complex in Q0119−046 and a similar complex in Q1115+080. For one of the systems, indirect arguments yield a distance $\Delta = 60$ kpc from the QSO. The most likely of several possible explanations for such complexes is that they arise from a (possibly collapsing) cluster of galaxies of which the QSO is a member. In Q0119−046, the "infall" velocities are on the borderline of being unreasonably high for such an origin. The high-velocity filaments in the NGC 1275 system may be similar to the clouds responsible for the $z_{abs} > z_{em}$ systems.

*Subject headings:* galaxies: clusters of — line identification — quasars

## I. INTRODUCTION

The Parkes radio source Q0119−046 was studied spectroscopically by Kinman and Burbidge (1967) who reported an emission redshift $z_{em} = 1.955 \pm 0.005$. They saw a strong absorption line system with a redshift $z_{abs} = 1.966$ that was distinctly larger than the emission redshift.

A subsequent, intermediate-resolution spectroscopic study of Q0119−046 and of six other QSOs with $z_{abs} > z_{em}$ was performed by Weymann *et al.* (1977, hereafter WWBM). This resolved the absorption line system at $z_{abs} = 1.966$ into three components between which there was apparently line locking amongst N V $\lambda\lambda$1238, 1242 doublets. Weymann *et al.* also discussed the origin of absorption systems with $z_{abs} > z_{em}$. They concluded that no single mechanism could account for the phenomenon; however, it was thought likely that gas clouds in a cluster around the quasar, on the one hand, and radiative acceleration of gas clouds by the QSO, on the other, were the most likely explanations.

In this paper, we present high-resolution, high signal-to-noise ratio data on Q0119−046. This enables us to make a detailed analysis of the absorption complex with $z_{abs} > z_{em}$ in Q0119−046 and to discuss the physical nature of such complexes in general. In this connection, we also discuss a similar absorption complex in Q1115+080 which was the subject of a recent paper (Young, Sargent, and Botsenberg 1982, hereafter YSB). We show that the observations suggest that the absorbing gas in the systems with $z_{abs} > z_{em}$ in these objects is $\geq 60$ kpc from the QSO, with equality holding for a cloud in the Q0119−046 complex.

## II. OBSERVATIONS AND REDUCTIONS

### a) Observations

The observations were made with the Las Campanas 100 inch (2.54 m) reflector and the Palomar 200 inch (5.08 m) reflector. The instrumental setups and modes of observation were exactly as described in YSB. A journal of observations of Q0119−046 is given in Table 1. All line wavelengths in this paper are heliocentric, vacuum values.

### b) Emission Lines

The emission lines of Ly$\alpha$ and C IV in Q0119−046 are severely mutilated by the strong absorption lines, as can be seen from Figure 1. The first redshift determination by Kinman and Burbidge (1967) found $z_{em} = 1.955 + 0.005$, but there was a discrepancy of over 5 Å in rest wavelength between Ly$\alpha$ and C IV. Subsequently, WWBM reported $z_{em} = 1.948 \pm 0.005$ from the Ly$\alpha$ line alone. Our own measurements are given in Table 2. The Ly$\alpha$ line is particularly difficult to measure both because of absorption and because of satellite N V emission. The Si IV +

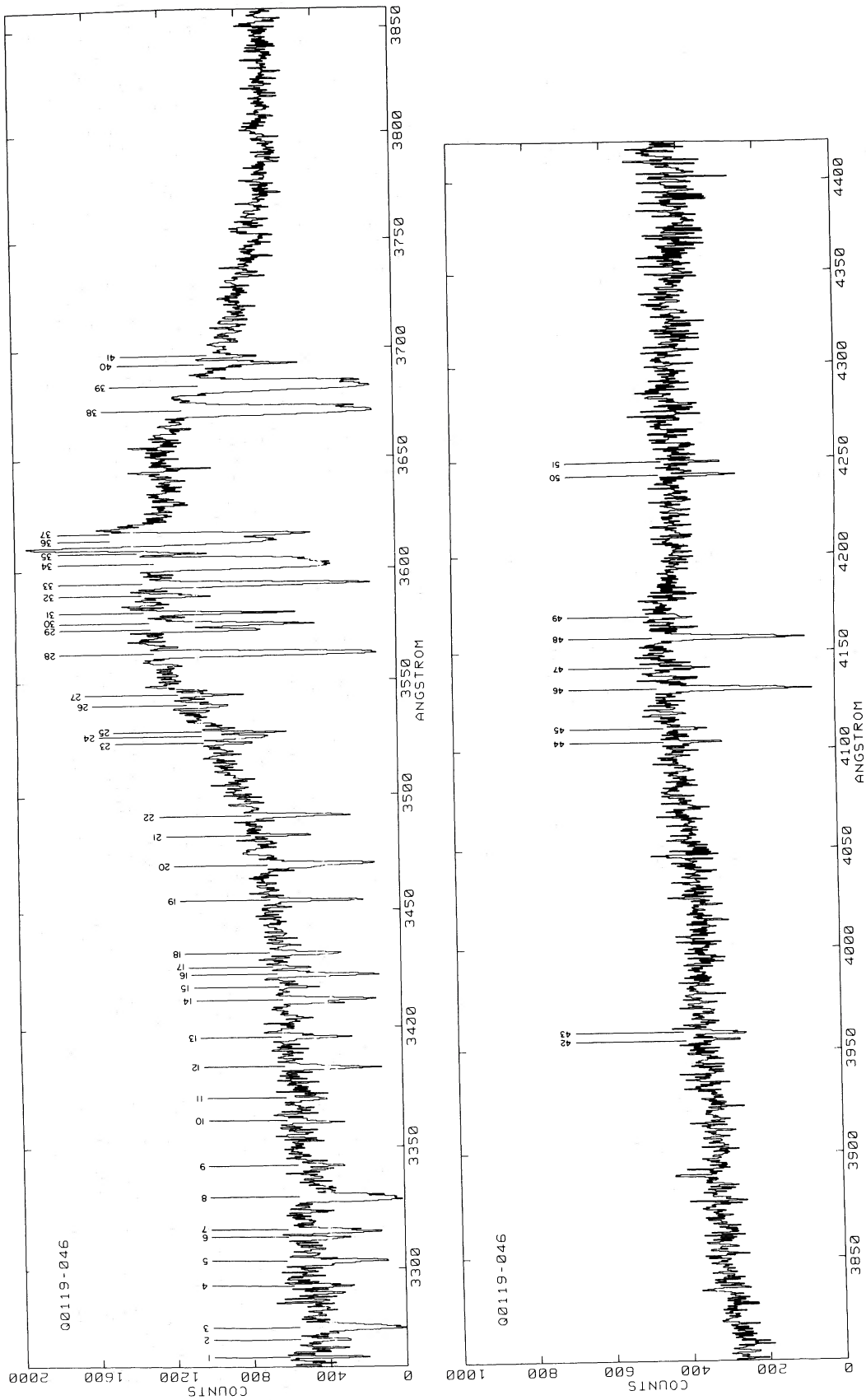


FIG. 1.—Spectra of Q0119−046. The first three spectra are from the 200 inch (5.08 m) and have 25.9 km s$^{-1}$ per data bin and a spectral resolution of 0.8 Å. The last spectrum is from the 100 inch (2.54 m) and has 72.4 km s$^{-1}$ per data bin and a resolution of 2.2 Å. The 61 absorption lines listed in Table 3 are marked. Slight rugosities are seen in the data at $\lambda$3889 because of afterglow from a helium lamp, and at $\lambda\lambda$4047, 4359 because of imperfect sky subtraction. The data are on a linearized flux scale whose "count" level bears no relation to the original data counts.

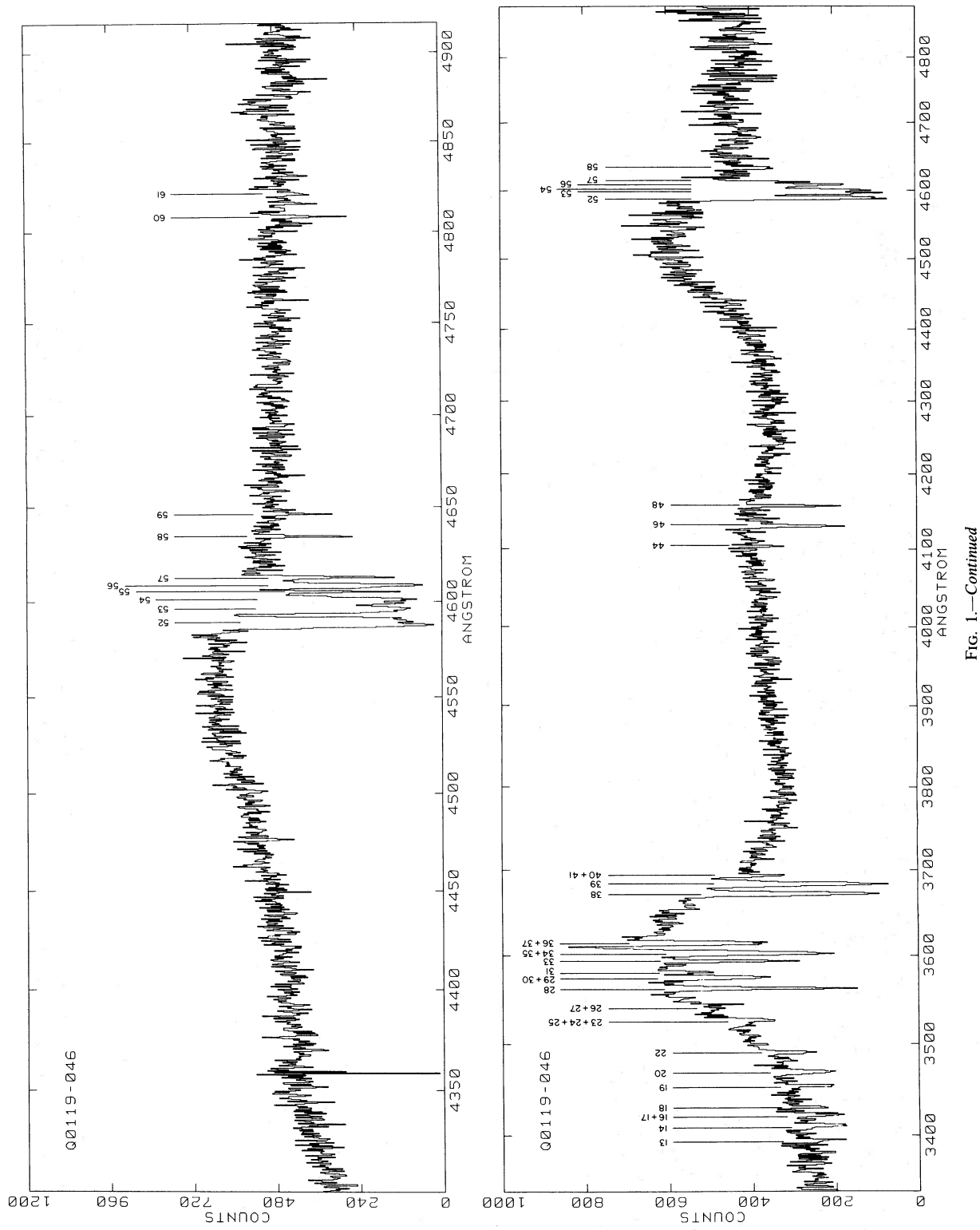


FIG. 1.—*Continued*

TABLE 1

OBSERVATIONS OF Q0119−046

| Date (1980) | UT Start | Time (s) | λ-Range (Å) | FWHM (Å) | Dispersion (Å mm$^{-1}$) | Telescope |
|---|---|---|---|---|---|---|
| Nov 10 | $00^h54^m$ | 8000 | 3340–4879 | 2.2 | 56 | C100 |
| Dec 1 | 04 00 | 10008 | 3801–4421 | 0.8 | 18 | P200 |
| Dec 2 | 02 31 | 9128 | 4300–4916 | 0.8 | 18 | P200 |
| Dec 3 | 02 21 | 11263 | 3260–3879 | 0.8 | 18 | P200 |

TABLE 2

EMISSION LINES IN Q0119−046

| Ion | $\lambda_{rest}$ (Å) | $\lambda_{obs}$ (Å) | $z_{em}$ | $W_{obs}$ (Å) | $W_{rest}$ (Å) |
|---|---|---|---|---|---|
| H I[a] | 1215.7 | 3588 ± 10 | 1.951 ± 0.008 | 199 ± 15 | 67.5 ± 5.1 |
| Si IV+O IV] | 1401.6[b] | 4117 ± 7 | 1.937 ± 0.005 | 20 ± 3 | 6.8 ± 1.0 |
| C IV | 1549.1 | 4550 ± 3 | 1.937 ± 0.002 | 88 ± 4 | 30.0 ± 1.4 |
| $\langle z_{em} \rangle$ | ... | ... | 1.937 ± 0.002 | ... | ... |

[a] Severely lacerated by strong absorption lines. Quantities unreliable.
[b] Assumes 85% O IV] λ1402.5 and 15% Si IV λ1396.8 as in Wills and Netzer 1979.

O IV] feature is also somewhat uncertain because of the unknown ratio of the two transitions comprising the line (it varies among QSOs; see Wills and Netzer 1979). However, it was possible to interpolate across the absorption in the red wing of the C IV emission to give a reliable line profile and redshift. In fact, the C IV and the Si IV + O IV] features agree in giving $z_{em} = 1.937$ which we adopt for the redshift of Q0119−046. The value for Lyα emission is appreciably larger than this, in accord with previous measurements. Note that the Lyα line in our high-resolution spectra shows a sharp emission feature at λ3610 which lies between two of the many strong absorption lines in this region of the spectrum. This emission line is not observed in the sky away from the spectrum of the QSO itself; we believe it to be an accidental feature resulting from the heavy absorption overlying the broad Lyα emission line.

### c) *Absorption Lines*

Seven absorption lines in a system with $z_{abs} = 1.966$ were discovered by Kinman and Burbidge (1967). The subsequent study by WWBM found 21 lines, including complex structure in the system at $z_{abs} = 1.966$. We have analyzed the spectrum with the procedures described in YSB and we present a list of 61 lines in Table 3 (some of these lines exhibit complex structure; this is described in the footnotes to Table 3). We show the four spectra of Q0119−046 in Figure 1 where the absorption lines are labeled. We found it difficult to estimate the continuum level around Lyα emission where the spectrum is severely lacerated by absorption. Equivalent widths of lines 31–37 are uncertain because of this problem.

The C100 and P200 spectra overlap. It is instructive to compare the two and to see how much gain is achieved by improving the spectral resolution from 2.2 Å to 0.8 Å.

## III. ABSORPTION LINE SYSTEMS

### a) *Metal Line Systems*

The analysis of the line list proceeded in the manner described in YSB. A total of seven absorption line systems were found as set out in Table 4. We comment on the individual systems as follows:

$z_{abs} = 0.6577$ (*System 1*). This is an isolated Mg II λλ2796, 2803 doublet. It is quite strong and leads to a certain redshift system. The lines are very narrow and are hardly resolved.

$z_{abs} = 0.7199$ (*System 2*). An isolated Mg II doublet. The lines are rather weak but the separation is correct. This is a probable system but not totally secure.

$z_{abs} = 1.6512$ (*System 3*). An isolated C IV λλ1548, 1550 doublet. The lines are definitely present and have the correct separation; this is a reasonably secure system.

$z_{abs} = 1.7403$ (*System 4*). A strong, isolated C IV doublet is seen longward of Lyα emission. There is a Lyα absorption in this system, but the wavelength discrepancy leads us to suspect that it is blended. A secure system, nevertheless.

$z_{abs} = 1.9644, 1.9655$ (*Systems 5A, 5B*). This is part of the absorption complex with $z_{abs} > z_{em}$. It has strong C IV λλ1548, 1550; N V λλ1238, 1242, and Si IV λλ1393, 1402 doublets, as well as C II λ1334 and excited fine structure C II* λ1335 lines. The line profiles of C IV, N V, and Lyα suggest the presence of at least two components, at $z_{abs} = 1.9644$ and 1.9655, of which the former is stronger. The Si IV, C II, C II*, and Si III λ1206 lines appear to be dominated by the $z_{abs} = 1.9644$ component, which itself seems to have substructure.

$z_{abs} = 1.9724$ (*System 6*). The central system in the $z_{abs} > z_{em}$ complex. The C IV λ1548 line is blended with

TABLE 3

Q0119−046 Absorption Line List

| No. | $\lambda_{obs}$ | $\sigma(\lambda)$ | $W_{obs}$ | $\sigma(W)$ | S/N | ID | $z_{abs}$ | S1 | S2 |
|---|---|---|---|---|---|---|---|---|---|
| 1 | 3265.10 | 0.08 | 0.42 | 0.06 | 9.3 | | | | |
| 2 | 3272.04 | 0.11 | 0.41 | 0.08 | 8.6 | | | | |
| 3 | 3276.99 | 0.09 | 2.37 | 0.13 | 8.5 | | | * | |
| 4 | 3293.94 | 0.09 | 0.60 | 0.08 | 10.0 | | | | * |
| 5 | 3304.01 | 0.08 | 1.53 | 0.09 | 10.9 | | | * | * |
| 6 | 3313.52 | 0.09 | 0.56 | 0.07 | 10.7 | | | | * |
| 7 | 3316.38 | 0.08 | 1.30 | 0.08 | 11.0 | | | * | * |
| 8 | 3329.88 | 0.07 | 3.05 | 0.10 | 12.0 | HI(1215) | 1.7391 | * | * |
| 9 | 3343.12 | 0.09 | 0.58 | 0.06 | 12.9 | | | | * |
| 10 | 3361.33 | 0.09 | 0.44 | 0.05 | 12.9 | | | | |
| 11 | 3370.90 | 0.10 | 0.36 | 0.06 | 12.9 | | | | |
| 12 | 3384.02 | 0.08 | 1.16 | 0.07 | 13.5 | | | * | * |
| 13 | 3396.91 | 0.11 | 0.76 | 0.07 | 15.1 | | | | * |
| 14 | 3412.54 | 0.07 | 1.56 | 0.06 | 17.6 | | | * | * |
| 14A | 3411.36 | .... | 0.40 | .... | 17.6 | | | | |
| 14B | 3412.95 | .... | 1.16 | .... | 17.6 | | | | |
| 15 | 3418.07 | 0.09 | 0.25 | 0.04 | 17.8 | | | | |
| 16 | 3423.38 | 0.07 | 1.30 | 0.05 | 18.6 | | | * | * |
| 17 | 3426.46 | 0.10 | 0.25 | 0.04 | 18.2 | | | | |
| 18 | 3432.39 | 0.08 | 0.80 | 0.05 | 18.1 | | | | * |
| 19 | 3455.21 | 0.07 | 0.93 | 0.05 | 19.2 | | | * | * |
| 20 | 3470.78 | 0.07 | 1.92 | 0.06 | 20.2 | | | * | * |
| 21 | 3483.46 | 0.07 | 0.34 | 0.03 | 20.5 | | | | |
| 22 | 3491.90 | 0.07 | 1.05 | 0.04 | 21.9 | | | * | * |
| 23 | 3523.67 | 0.10 | 0.25 | 0.03 | 24.6 | | | | |
| 24 | 3526.41 | 0.08 | 0.58 | 0.04 | 24.8 | | | | * |
| 25 | 3528.39 | 0.07 | 0.42 | 0.03 | 25.6 | | | | |
| 26 | 3540.18 | 0.10 | 0.35 | 0.03 | 26.2 | | | | |
| 27 | 3544.93 | 0.09 | 0.35 | 0.03 | 26.2 | | | | |
| 28 | 3563.22 | 0.06 | 2.36 | 0.04 | 26.2 | | | * | * |
| 29 | 3574.09 | 0.07 | 0.77 | 0.03 | 27.9 | | | | |
| 30 | 3576.63 | 0.07 | 1.34 | 0.04 | 26.9 | SiIII(1206) | 1.9644 | | |
| 31 | 3581.62 | 0.07 | 0.76 | 0.03 | 28.4 | | | | |
| 32 | 3589.52 | 0.09 | 0.41 | 0.03 | 28.4 | SiIII(1206) | 1.9751 | | |
| 33 | 3594.48 | 0.07 | 1.95 | 0.04 | 28.6 | | | | |
| 34 | 3603.49 | 0.07 | 4.54 | 0.05 | 32.2 | HI(1215) | 1.9642 | | |
| 35 | 3608.45 | 0.06 | 0.85 | 0.02 | 32.9 | | | | |
| 36 | 3613.57 | 0.06 | 2.17 | 0.03 | 31.6 | HI(1215) | 1.9725 | | |
| 37 | 3616.43 | 0.06 | 1.60 | 0.03 | 30.9 | HI(1215) | 1.9748 | | |
| 38 | 3672.80 | 0.07 | 4.06 | 0.05 | 28.4 | NV(1238) | 1.9648 | | |
| 38A | 3672.14 | .... | .... | .... | 28.4 | | | | |
| 38B | 3674.27 | .... | .... | .... | 28.4 | | | | |
| 39 | 3684.10 | 0.07 | 4.51 | 0.05 | 29.5 | NV(1242) | 1.9644 | | |
| 39A | 3683.58 | .... | .... | .... | 29.5 | | | | |
| 39B | 3685.92 | .... | .... | .... | 29.5 | | | | |
| 40 | 3694.04 | 0.07 | 0.91 | 0.04 | 28.9 | NV(1242) | 1.9724 | | |
| 41 | 3697.68 | 0.09 | 0.40 | 0.03 | 27.1 | NV(1242) | 1.9753 | | |
| 42 | 3956.06 | 0.10 | 0.23 | 0.04 | 15.3 | CII(1334) | 1.9644 | | |
| 43 | 3959.46 | 0.12 | 0.41 | 0.06 | 15.2 | CII*(1335) | 1.9643 | | |
| 44 | 4104.56 | 0.14 | 0.38 | 0.06 | 17.5 | CIV(1548) | 1.6512 | | |
| 45 | 4111.54 | 0.12 | 0.24 | 0.05 | 16.8 | CIV(1550) | 1.6513 | | |
| 46 | 4131.67 | 0.08 | 1.82 | 0.08 | 16.1 | SiIV(1393) | 1.9644 | | |
| 47 | 4142.59 | 0.12 | 0.38 | 0.06 | 16.5 | SiIV(1393) | 1.9722 | | |
| 48 | 4158.39 | 0.09 | 1.73 | 0.08 | 16.0 | SiIV(1402) | 1.9644 | | |
| 49 | 4169.09 | 0.17 | 0.31 | 0.06 | 16.8 | SiIV(1402) | 1.9720 | | |
| 50 | 4242.60 | 0.09 | 0.46 | 0.05 | 15.6 | CIV(1548) | 1.7403 | | |
| 51 | 4249.51 | 0.09 | 0.31 | 0.05 | 16.0 | CIV(1550) | 1.7403 | | |
| 52 | 4589.83 | 0.07 | 5.00 | 0.10 | 18.6 | CIV(1548) | 1.9646 | | |
| 53 | 4597.67 | 0.07 | 4.53 | 0.10 | 16.8 | CIV(1550) | 1.9648 | | |
| 54 | 4602.36 | 0.07 | 2.43 | 0.08 | 16.7 | CIV(1548) | 1.9727 | | |
| 55 | 4606.06 | 0.08 | 1.03 | 0.06 | 16.6 | CIV(1548) | 1.9751 | | |
| 56 | 4609.58 | 0.08 | 2.50 | 0.09 | 15.9 | CIV(1550) | 1.9724 | | |
| 57 | 4613.64 | 0.08 | 1.17 | 0.07 | 15.5 | CIV(1550) | 1.9751 | | |
| 58 | 4635.53 | 0.09 | 0.50 | 0.06 | 15.4 | MgII(2796) | 0.6577 | | |
| 59 | 4647.52 | 0.14 | 0.37 | 0.07 | 14.4 | MgII(2803) | 0.6577 | | |
| 60 | 4809.50 | 0.11 | 0.46 | 0.07 | 13.0 | MgII(2796) | 0.7199 | | |
| 61 | 4821.94 | 0.18 | 0.32 | 0.08 | 13.5 | MgII(2803) | 0.7200 | | |

Notes.—Region observed from 3260 Å to 4916 Å. All wavelengths vacuum, heliocentric values. Starred lines are H I ($\lambda$1215) samples. Lines 14, 38, and 39 seem double, and we have listed the approximate wavelengths of the components. Lines 52 and 53 exhibit a complicated structure which defies a unique splitting into components.

TABLE 4

Q0119−046 ABSORPTION SYSTEMS

| No. | Ion | $\lambda_{rest}$ | $\lambda_{calc}$ | $\lambda_{obs}$ | O-C | $z_{abs}$ | $W_{obs}$ | $W_{rest}$ | Comments |
|---|---|---|---|---|---|---|---|---|---|
| 1 | Mg II | 2803.53 | 4647.41 | 4647.52 | +0.11 | 0.6577 | 0.37 | 0.22 | |
| | Mg II | 2796.35 | 4635.51 | 4635.53 | +0.02 | 0.6577 | 0.50 | 0.30 | |
| | | | | | <z> = | 0.6577 | | | |
| 2 | Mg II | 2803.53 | 4821.79 | 4821.94 | +0.15 | 0.7200 | 0.32 | 0.19 | |
| | Mg II | 2796.35 | 4809.44 | 4809.50 | +0.06 | 0.7199 | 0.46 | 0.27 | |
| | | | | | <z> = | 0.7199 | | | |
| 3 | C IV | 1550.77 | 4111.40 | 4111.54 | +0.14 | 1.6513 | 0.24 | 0.09 | |
| | C IV | 1548.20 | 4104.59 | 4104.56 | -0.03 | 1.6512 | 0.38 | 0.14 | |
| | | | | | <z> = | 1.6512 | | | |
| 4 | H I | 1215.67 | 3331.30 | 3329.88 | -1.42 | 1.7391 | 3.05 | 1.11 | Probably blended. |
| | C IV | 1550.77 | 4249.58 | 4249.51 | -0.07 | 1.7403 | 0.31 | 0.11 | |
| | C IV | 1548.20 | 4242.53 | 4242.60 | +0.07 | 1.7403 | 0.46 | 0.17 | |
| | | | | | <z> = | 1.7403 | | | |
| | Multiple system. Obvious components at z = 1.9644, 1.9655. | | | | | | | | |
| 5 | H I | 1215.67 | 3603.98 | 3603.49 | -0.49 | 1.9642 | 4.54 | 1.53 | |
| | C II | 1334.53 | 3956.35 | 3956.06 | -0.29 | 1.9644 | 0.23 | 0.08 | |
| | C II* | 1335.70 | 3959.82 | 3959.46 | -0.36 | 1.9643 | 0.41 | 0.14 | |
| | C IV | 1550.77 | 4597.41 | 4597.67 | +0.26 | 1.9648 | 4.53 | 1.53 | Embedded in complex. |
| | C IV | 1548.20 | 4589.79 | 4589.83 | +0.04 | 1.9646 | 5.00 | 1.69 | |
| | N V | 1242.80 | 3684.40 | 3684.10 | -0.30 | 1.9644 | 4.51 | 1.52 | Embedded in complex. |
| | N V | 1238.82 | 3672.61 | 3672.80 | +0.19 | 1.9648 | 4.06 | 1.37 | |
| | Si III | 1206.51 | 3576.82 | 3576.63 | -0.19 | 1.9644 | 1.34 | 0.45 | |
| | Si IV | 1402.77 | 4158.65 | 4158.39 | -0.26 | 1.9644 | 1.73 | 0.58 | |
| | Si IV | 1393.76 | 4131.94 | 4131.67 | -0.27 | 1.9644 | 1.82 | 0.61 | |
| | | | | | <z> = | 1.9646 | | | |
| 6 | H I | 1215.67 | 3613.46 | 3613.57 | +0.11 | 1.9725 | 2.17 | 0.73 | |
| | C IV | 1550.77 | 4609.51 | 4609.58 | +0.07 | 1.9724 | 2.50 | 0.84 | |
| | C IV | 1548.20 | 4601.87 | 4602.36 | +0.49 | 1.9727 | 2.43 | 0.82 | Embedded in complex. |
| | N V | 1242.80 | 3694.10 | 3694.04 | -0.06 | 1.9724 | 0.91 | 0.31 | |
| | Si IV | 1402.77 | 4169.59 | 4169.09 | -0.50 | 1.9720 | 0.31 | 0.10 | |
| | Si IV | 1393.76 | 4142.81 | 4142.59 | -0.22 | 1.9722 | 0.38 | 0.13 | |
| | | | | | <z> = | 1.9724 | | | |
| 7 | H I | 1215.67 | 3616.74 | 3616.43 | -0.31 | 1.9748 | 1.60 | 0.54 | |
| | C IV | 1550.77 | 4613.70 | 4613.64 | -0.06 | 1.9751 | 1.17 | 0.39 | |
| | C IV | 1548.20 | 4606.05 | 4606.06 | +0.01 | 1.9751 | 1.03 | 0.35 | Embedded in complex. |
| | N V | 1242.80 | 3697.45 | 3697.68 | +0.23 | 1.9753 | 0.40 | 0.13 | |
| | Si III | 1206.51 | 3589.49 | 3589.52 | +0.03 | 1.9751 | 0.41 | 0.14 | |
| | | | | | <z> = | 1.9751 | | | |

the C IV doublet of system 5. A similar situation obtains with the N V $\lambda$1238 line. There is a weak Si IV doublet and a strong Ly$\alpha$ line to complete this system. The appearance of the N V and C IV lines suggests the presence of substructure within this system.

$z_{abs} = 1.9751$ (*System 7*). This is the highest redshift seen in Q0119−046 and has C IV, Ly$\alpha$, and Si III $\lambda$1206 present. The N V $\lambda$1242 line is found, but the N V $\lambda$1238 line is blended in the red wing of N V $\lambda$1242 of system 5.

As usual, only systems with lines longward of Ly$\alpha$ emission attain low enough chance coincidence probabilities to be deemed real. A hunt for Mg II $\lambda\lambda$2796, 2803 doublets below Ly$\alpha$ emission found a possibility at $z_{abs} = 0.2243$ with lines 16 and 18 in Table 3. The line widths are similar, the separation is correct to 0.22 Å, and the equivalent width ratio quite reasonable. No other lines were seen in this system which, therefore, remains only a possible one.

### *b) Ly$\alpha$ Only Systems*

Most of the lines above Ly$\alpha$ emission were identified in one of the metal line absorption systems. As usual, very few lines in the forest below Ly$\alpha$ emission could be identified. Most of the remainder are solitary Ly$\alpha$ absorption lines. In YSB, we analyzed new samples of Ly$\alpha$ lines including those from Q0119−046. Asterisks in Table 3 define the samples used in YSB; we refer to that work for details of the selection criteria and for the analysis of the Ly$\alpha$ samples.

## IV. ION COLUMN DENSITIES

### *a)* Mg II: *System 1*

We shall obtain column densities and velocity structure information for the stronger absorption systems in Q0119−046 in the manner described in YSB. The first set of lines with a good enough signal-to-noise ratio for such analysis is the Mg II $\lambda\lambda$2796, 2803 doublet at $z_{abs} = 0.6577$. It is depicted in Figure 2 on an enlarged scale; the lines seem to consist of a central, narrow core superposed on a broader absorption feature. For the central core, we measure rest equivalent widths

$$W_1 = 0.128 \pm 0.014 \text{ Å}, \quad W_2 = 0.228 \pm 0.014 \text{ Å}, \quad (1)$$

to give a doublet ratio $R = 1.78 \pm 0.22$. The lines have essentially the width of the instrumental profile ($\sigma = 20$ km s$^{-1}$), and so line fitting will yield little information other than the fact that $\sigma_v < 12$ km s$^{-1}$ for the line-of-sight velocity dispersion in the absorbing cloud [here, we define $\sigma_v$ such that the velocity distribution function is $\Psi(v) = \exp(-v^2/2\sigma_v^2)/\sigma_v(2\pi)^{1/2}$].

We find, from considering the doublet ratio and its estimated error that,

$$8 < \sigma_v < 12 \text{ km s}^{-1}, \quad \log N_i = 12.86 \pm 0.05 . \quad (2)$$

In Figure 2, we see the lines also seem to have a broad wing component, displaced 15 km s$^{-1}$ longward of the central core. For this, the rest equivalent widths are

$$W_1 = 0.084 \pm 0.028 \text{ Å}, \quad W_2 = 0.152 \pm 0.028 \text{ Å} . \quad (3)$$

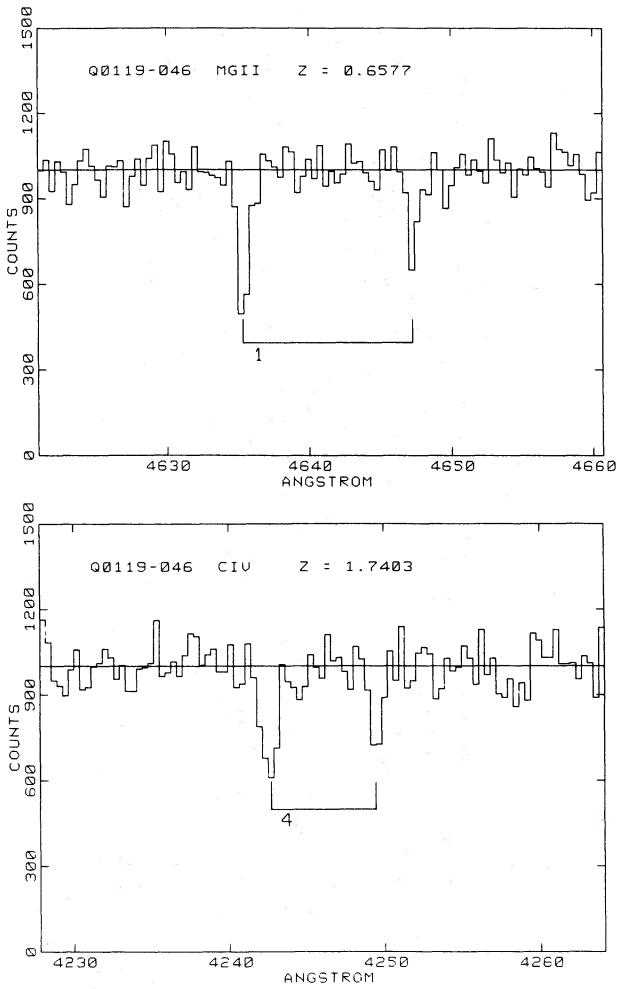


FIG. 2.—The Mg II lines in $z_{abs} = 0.6577$ and the C IV lines in $z_{abs} = 1.7403$ in Q0119−046. The doublets are marked with the redshifts system number in Table 4. Each data bin is 25.9 km s$^{-1}$ and the spectral resolution is 0.8 Å. The spectra have been divided by the continuum levels, shown as a horizontal line.

The doublet ratio is consistent with the value of 2 corresponding to the optically thin case. Since these wings are well resolved, it must be optically thin and undamped (unless it consists of a picket fence of sharp, saturated components). In the Gaussian cloud approximation, the observed line width gives,

$$\sigma_v = 55 \pm 10 \text{ km s}^{-1}, \quad (4)$$

and the equivalent width yields

$$\log N_i = 12.61 \pm 0.11 . \quad (5)$$

### *b)* C IV: *System 4*

This is an isolated C IV $\lambda\lambda$1548, 1550 doublet which is shown on an enlarged scale in Figure 2. The doublet ratio $R = 1.48$ will, within the errors, admit either damped or undamped solutions. Profile fitting yields the best undamped solution as

$$\sigma_v = 13 \pm 3 \text{ km s}^{-1}, \quad \log N_i = 13.89 \pm 0.04 . \quad (6)$$

The damped solution, although technically consistent with the data, is rejected as being implausible. This is because (i) no other lines are seen in this absorption system, and (ii) the required velocity dispersion $\sigma_v < 1.5$ km s$^{-1}$ is too small for plausible cloud temperatures.

*c*) C II: *System 5A*

In Figure 3, the C II $\lambda$1334 and C II* $\lambda$1335 lines are shown on an expanded scale. The $z_{abs} = 1.9646$ systems shows at least two distinct components, and the C II lines are from the component at $z_{abs} = 1.9644$ (system 5A) only. The line attributed to C II* $\lambda$1335 cannot be attributed to any other line in the known redshift systems in Q0119−046. The ratio of the lines is $R = 1.78$, where $R = 2$ is expected for optically thin lines with a fully populated, upper, fine structure state. Our observations are compatible with ratios in the range $R = 1.5$–2.0.

The resulting, optically thin column densities are

$$\log N(\text{C II}) = 13.62 \pm 0.08 ,$$
$$\log N(\text{C II*}) = 13.87 \pm 0.08 . \quad (7)$$

According to the work of Bahcall and Wolf (1968) on the collisional population of fine structure states of C II, our ratio of $N$(C II*)/$N$(C II) demands gas densities $n(\text{H}) > 100$ cm$^{-3}$ if the hydrogen is ionized and $n(\text{H}) > 5 \times 10^3$ cm$^{-3}$ if the hydrogen is neutral. The former case is obviously most plausible in view of the high-ionization state of this redshift system.

*d*) Si IV: *Systems 5A, 6*

The Si IV $\lambda\lambda$1393, 1402 lines in the $z_{abs} = 1.97$ complex are relatively uncomplicated as may be seen in Figure 3. The lines in $z_{abs} = 1.9724$ (system 6) are quite weak but seem quite wide and resolved. The doublet ratio $R = 1.22 \pm 0.57$ is not well determined because of the weakness of the lines: an unsaturated ratio of $R = 2$ is compatible with the observations. The optically thin column density is

$$\log N_i = 13.7 \pm 0.1 , \quad (8)$$

and the line widths correspond to a dispersion $\sigma_v \approx 60$ km s$^{-1}$.

The lines of Si IV in the $z_{abs} = 1.9644$ (system 5A) are strong, and the doublet ratio is $R = 1.05 \pm 0.06$, indicating that the lines are on the logarithmic part of the curve of growth. Inspection of the line profiles in Figure 3 shows that a one-cloud model will not suffice. Both Si IV lines have a small plateau just longward of the line center indicating a second, weaker cloud on the verge of being resolved. A low column density solution was found with two clouds having the following properties (commas separate the values for the two clouds):

$$\sigma_v = 19.3, 9.7 \quad (\text{km s}^{-1}) ;$$
$$\log N_i = 14.70, 14.00 ;$$
$$v = 0, +70 \quad (\text{km s}^{-1}) ; \quad (9)$$

giving a total column density $\log N_i = 14.48$. We show the corresponding fit in Figure 4. The redshift of the Si IV lines indicates that they are in system 5A ($z_{abs} = 1.9644$) and the system 5B ($z_{abs} = 1.9655$) shows no Si IV. The two-cloud model required for Si IV indicates that the $z_{abs} = 1.9644$ component itself has substructure. We may augment the column densities of the model by decreasing the velocity dispersions; since the lines are on the logarithmic part of the curve of growth, there is considerable uncertainty in column density. Accordingly, we evolved a second model with the following properties:

$$\sigma_v = 4.8, 2.4 \quad (\text{km s}^{-1}) ;$$
$$\log N_i = 17.09, 16.79 ;$$
$$v = 0, +77 \quad (\text{km s}^{-1}) ; \quad (10)$$

with a total column density $\log N_i = 17.25$. This solution also fits the data, as shown in Figure 4. There are perceptible damping wings on the lines for which slight evidence exists in the data. We believe the total column densities of equations (9) and (10) represent the maximum range admitted by the observations.

*e*) Si III: *Systems 5A, 7*

In Figure 3, we show the Si III $\lambda$1206 lines in the $z_{abs} = 1.97$ absorption complex. Only systems 5A and 7 at $z_{abs} = 1.9644$ and 1.9751 have a Si III line visible, the former being much stronger. Since it is not a doublet, column densities for Si III are difficult to determine. However, in system 7, the line is weak, and, if represented by a Gaussian cloud, it is optically thin. Then, we find

$$\sigma_v = 75 \pm 10 \text{ km s}^{-1} , \quad \log N_i = 12.82 \pm 0.05 . \quad (11)$$

If the structure is more complicated, equation (11) represents a lower limit to the column density. The column density of Si III in system 5A is almost indeterminate since the velocity structure of the system cannot be obtained. The line is well resolved and not particularly deep, which favors low column densities if a single Gaussian cloud model is employed. In that case, direct measurement gives

$$\sigma_v = 60 \pm 10 \text{ km s}^{-1} , \quad \log N_i = 13.5 \pm 0.1 . \quad (12)$$

This is also close to the column density that the two-cloud model in Si IV given in equation (9) would yield. If the line is comprised of narrow, highly saturated components, as in the Si IV model represented by equation (10), then the column density may be up to $\log N_i \approx 17.0$. Above this value, the line develops strong damping wings which are not observed.

*f*) Ly$\alpha$: *Systems 5A, 5B, 6, 7*

The Ly$\alpha$ absorption occurs in systems 5A, 5B, 6, and 7 of the $z_{abs} = 1.97$ complex, as may be seen in Figure 3. The lines are very wide and yet do not reach anywhere close to zero intensity in their centers. This suggests that either they are optically thin with huge velocity dispersions, or they are comprised of a picket fence of saturated components which are unresolved. There is no way, from the given data, to decide upon the actual velocity structure of

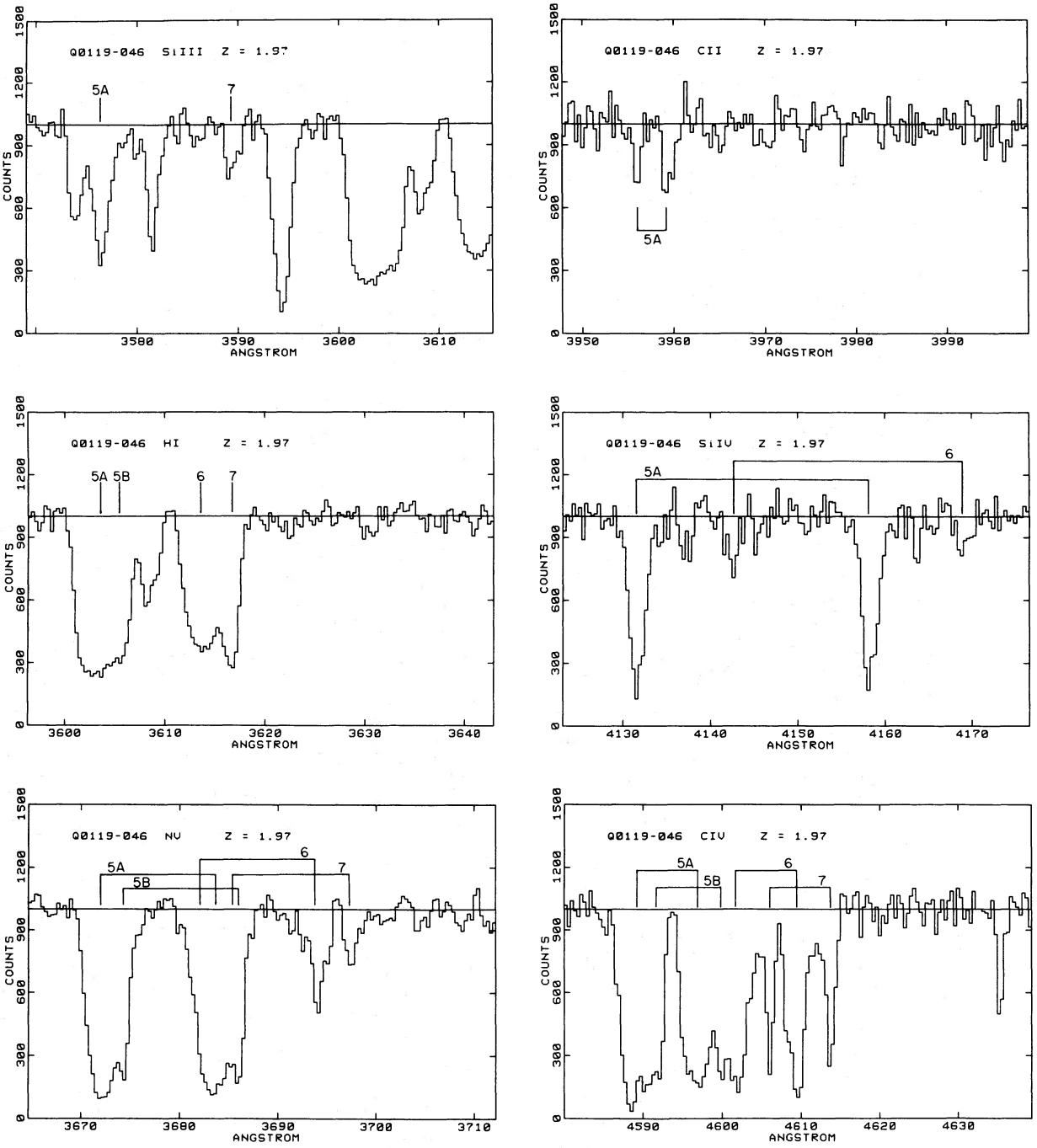


FIG. 3.—The $z_{abs} = 1.97$ absorption complex in Q0119−046. We show the data on six lines and doublets and have marked the redshift systems 5A, 5B, 6, and 7 as given in Table 4. Each data bin is 25.9 km $s^{-1}$ and the spectral resolution is 0.8 Å. The spectra have been divided by the continuum levels, shown as horizontal lines.

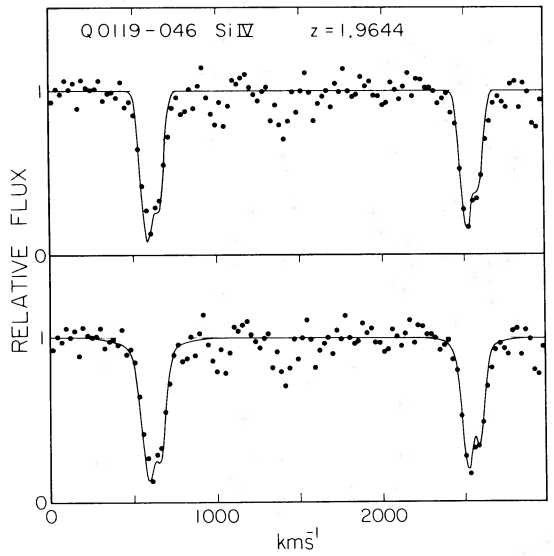


FIG. 4.—Profile fits to the Si IV λλ1393, 1402 lines in the $z_{abs} = 1.9646$ absorption system in Q0119−046. The top graph shows an undamped, two-cloud model. The bottom graph is a damped, two-cloud model with nearly 1000 times the ionic column density of the top model. Full details are given in § IV*d*.

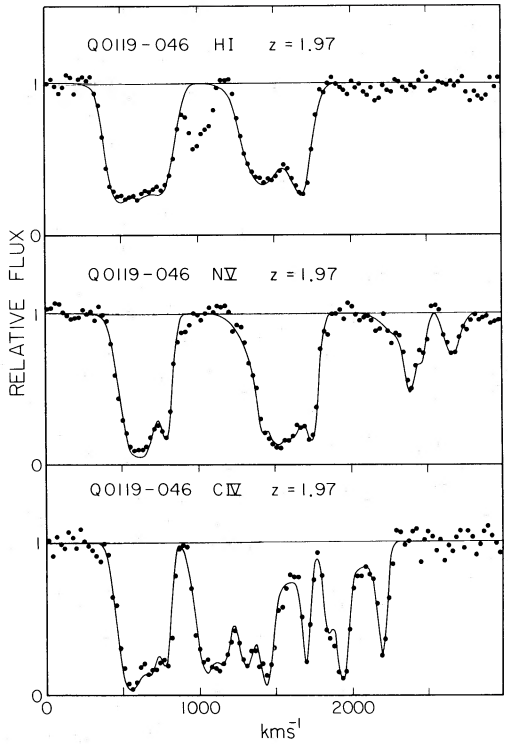


FIG. 5.—Profile fits to the $z_{abs} = 1.97$ complex in Q0119−046. We show multi-cloud models fitted to the Lyα, N V λλ1238, 1242, and C IV λλ1548, 1550 lines. These are the minimum column density solution as described in § IV.

the clouds, so we shall limit ourselves to computing minimum and maximum column densities. Added complications for the Lyα lines are:

1. The continuum in the region of the severely lacerated Lyα emission line is not reliably determined.

2. The fact that wide lines are not black in the center may be because they do not cover the entire emission line region of the QSO.

Although the Lyα lines are not centrally black, the corresponding C IV absorption (embedded in C IV emission) is very nearly black, and it is thus likely that the Lyα absorption does indeed cover the QSO Lyα emission region. We shall, therefore, ignore this second possibility in determining our column densities.

Minimum column densities were computed by fitted multiple Gaussian clouds to the line profiles of Lyα absorption lines as shown in Figure 3. The results are:

$$\begin{aligned} 5A&: z_{abs} = 1.9644\,, \quad \log N_i = 14.53\,; \\ 5B&: z_{abs} = 1.9655\,, \quad \log N_i = 14.14\,; \\ 6&: z_{abs} = 1.9724\,, \quad \log N_i = 14.36\,; \\ 7&: z_{abs} = 1.9751\,, \quad \log N_i = 14.18\,; \end{aligned} \tag{13}$$

and we show the line profile of the specific model that generated these column densities in Figure 5. We do not give more details for the model since it is the solution of an ill-conditioned problem and is not, therefore, a reliable indication of the true properties of the absorbing clouds.

Maximum column densities are limited by the appearance of damping wings on the line profiles. There is some danger in the present case, since the determination of the continuum level around the Lyα emission in Q0119−046 is rather uncertain. Nevertheless, the maximum values are $\log N_i \approx 18.5$ for the systems 5A + 5B and 6, and $\log N_i \approx 17.6$ for system 7. It would require a peculiar velocity structure (a picket fence of highly saturated lines) in order for these column densities to obtain without making the observed Lyα lines black in the center.

### *g*) N V: *Systems 5A, 5B, 6, 7*

Absorption lines due to N V λλ1238, 1242 are found in all four redshift systems 5A, 5B, 6, and 7 in the complex. They may be inspected in Figure 3. The N V doublet provides the clearest evidence that system 5 ($z_{abs} = 1.9646$) is split into two components 5A, 5B ($z_{abs} = 1.9644$, 1.9655). The configuration observed at lower resolution was suggested by WWBM as being possibly due to line locking since the N V λ1238 lines of systems 6 and 7 fall on the N V λ1242 lines of systems 5A and 5B. It seems to us inevitable that, if several redshift systems are randomly cast down with a velocity spread of $\sim 1000$ km s$^{-1}$, then apparent examples of "line locking" as good as those observed in these N V lines will almost certainly be seen in some doublet or other. For example, in the complex Q1115+080 (see YSB) the C IV λλ1548, 1550 lines exhibit some overlap between different redshifts. Accordingly, we do not regard the observed confluence of the N V lines in Q0119−046 as being evidence for this controversial phenomenon.

The N V λ1242 lines in system 6 and 7 are weak and are optically thin (unless the velocity structure of the clouds is peculiar). The line in system 6 seems to have a strong blue wing, indicating a multicomponent cloud structure.

Obtaining a satisfactory profile fit was not easy, and we finally settled on the following column densities:

$$\begin{aligned} 5A&: z_{abs} = 1.9644 , \quad \log N_i = 15.14 ; \\ 5B&: z_{abs} = 1.9655 , \quad \log N_i = 15.06 ; \\ 6&: z_{abs} = 1.9724 , \quad \log N_i = 14.72 ; \\ 7&: z_{abs} = 1.9751 , \quad \log N_i = 14.23 . \end{aligned} \tag{14}$$

The specific model that generated these column densities is shown fitted to the data in Figure 5. We do not give the full details of the Gaussian clouds used to generate this profile since the complexity of the meshing N v doublets makes the model ambiguous. Rather, the example given in equation (15) should be used as a guide to the minimum column densities that the data will allow. If the systems contain heavily saturated, narrow components, the column densities may be much higher (see Boksenberg, Carswell, and Sargent 1979).

Maximum column densities are limited by the strength of the damping wings on the line profiles. Trials with various cloud parameters lead to upper limits log $N_i \approx 18.6$ for all the systems 5A, 5B, 6, and 7.

*h*) C IV: *Systems 5A, 5B, 6, 7*

The C IV $\lambda\lambda$1548, 1552 doublet is found in all absorption systems in the $z_{abs} = 1.97$ complex, as may be seen in Figure 3. The lines are blended as well as being on the logarithmic part of the curve of growth, so that column densities are particularly difficult to determine for these lines. As for the other transitions in the $z_{abs} = 1.97$ complex, we have sought a low column density solution which resulted in the following values:

$$\begin{aligned} 5A&: z_{abs} = 1.9644 , \quad \log N_i = 15.03 ; \\ 5B&: z_{abs} = 1.9655 , \quad \log N_i = 14.66 ; \\ 6&: z_{abs} = 1.9724 , \quad \log N_i = 15.21 ; \\ 7&: z_{abs} = 1.9751 , \quad \log N_i = 15.39 ; \end{aligned} \tag{15}$$

and we show the model that generated these values in Figure 5. Once again, we supress the full details of the model since the complexity of meshing C IV doublets makes the individual cloud properties uncertain. Maximum column densities, from limits on the damping wings, are log $N_i = 18.4$, 17.4, 18.7, 18.1 for systems 5A, 5B, 6, and 7 respectively.

## V. THE ABSORPTION LINE COMPLEXES

*a*) *Properties of the $z_{abs} = 1.97$ Complex in Q0119−046*

There are four main absorption systems, some with substructure, with velocities relative to the QSO of:

$$\begin{aligned} 5A&: z_{abs} = 1.9644 , \quad v = -2780 \text{ km s}^{-1} ; \\ 5B&: z_{abs} = 1.9655 , \quad v = -2890 \text{ km s}^{-1} ; \\ 6&: z_{abs} = 1.9724 , \quad v = -3590 \text{ km s}^{-1} ; \\ 7&: z_{abs} = 1.9751 , \quad v = -3870 \text{ km s}^{-1} . \end{aligned} \tag{16}$$

These velocities are uncertain by about 200 km s$^{-1}$, which is the 1 $\sigma$ error on the emission redshift of Q0119−046 (see Table 2).

We note that the emission redshift of the QSO may differ by up to 3000 km s$^{-1}$ from that of the underlying structure. This is indicated by the difference in permitted and forbidden line redshifts in Seyfert galaxies. The large infall velocities given in equation (16) could possibly be illusory.

The ionization parameter (McKee, Tarter, and Weisheit 1973) for these systems may be judged by the column densities given in § III. Photoionization calculations seem to fit better than collision ionization because of the strength of the Ly$\alpha$ absorption and because (in $z_{abs} = 1.9644$) the C II and N V lines are both detectable. An acceptable ionization parameter is

$$\Upsilon = n(\text{H})/n_\gamma = 100$$

for $z_{abs} = 1.9655$ and 1.9724 where Si III $\lambda$1206 is not seen. The system $z_{abs} = 1.9751$ has Si III visible and N V weak, suggesting $\Upsilon = 300$. The system $z_{abs} = 1.9644$ has weak C II $\lambda$1334, and $\Upsilon = 300$ would also fit this system, which has considerably stronger lines than $z_{abs} = 1.9751$.

Let us examine the ionization structure of the $z_{abs} = 1.9644$ system in more detail. In Table 5, we give, for the observed ion species $X$, the quantities log $n(X)/n(\text{H})$ as deduced from the calculations of McKee, Tarter, and Weisheit (1973) with $\Upsilon = 300$. We also give the observed column densities log $N(X)$ or ranges thereof when $N(X)$ is ill-determined. The absolute value of $N$(C II + C II*) is correctly fitted for a total column density log $N(\text{H}) = 19.61$. We give, therefore, the quantities log $N(X) - 19.61$ in Table 5 which should be compared with the theoretical values. The quantity $\Upsilon = 300$ is quite sharply defined between the sharp decrease in $n$(C II + C II*) as $\Upsilon$ is lowered, and the sharp decrease in $n$(N V) as $\Upsilon$ is augmented.

Three assumptions are made for the purposes of comparing the theoretical calculations with observations:

1. The cloud is homogeneous.
2. The cloud is optically thin.
3. The QSO ionization radiation has an intensity $I_\nu = I_{\nu_c}(\nu/\nu_c)^{-3/2}$ from the Lyman continuum frequency $\nu_c$ up to energies of at least 100 eV.

Point (1) is highly unlikely to be true. Since $\Upsilon = n(\text{H})/n_\gamma$, and $n_\gamma$ is probably constant, the values of $\Upsilon$

TABLE 5

Q0119−046: IONIZATION STRUCTURE OF $z_{abs} = 1.9644$

| Ion ($X$) | $\Upsilon = 300$ log $n(X)/n$(H) | Observed log $N(X)$[a] | Observed log $N(X)$−19.61[a] |
|---|---|---|---|
| H I ..... | −3.18 | 14.53 to 18.50 | −5.08 to −1.11 |
| C II+C II* ... | −5.55 | 14.06 | −5.55 |
| C IV ..... | −3.72 | 15.03 to 18.40 | −4.58 to −1.21 |
| N V..... | −4.63 | 15.14 to 18.60 | −4.47 to −1.01 |
| Si III ..... | −5.09 | 13.50 to 17.00 | −6.11 to −2.61 |
| Si IV ..... | −4.44 | 14.48 to 17.25 | −5.13 to −2.36 |

[a] When a large range is given, values to the smaller end of the range are generally preferred (see § IV).

reflect variations in density. Suppose, for example, the cloud has values of $\Upsilon$ spread with a uniform distribution in logarithmic space. Writing

$$f_{\rm H\,I}(\Upsilon) = n({\rm H\ I};\ \Upsilon)/n({\rm H})\,, \tag{17}$$

we find from McKee, Tarter, and Weisheit (1973) that

$$f_{\rm H\,I}(\Upsilon) = f_{\rm H\,I}(300)(\Upsilon/300)^{4/5} \tag{18}$$

for values of $\Upsilon$ near 300. In that case, the effective value of $f$ is,

$$\langle f_{\rm H\,I}\rangle = \frac{\int f_{\rm H\,I}(\Upsilon) d\ \ln \Upsilon}{\int d\ \ln \Upsilon} \tag{19}$$

for the supposed case. If the range of $\Upsilon$ is from 100 to 1000, say, then $\langle f_{\rm H\,I}\rangle = 2.76 f_{\rm H\,I}(300)$. In that case, as expected, one sees more H I than one would using the mean value $\langle\Upsilon\rangle$ to compute $n$(H I). For the C II ion;

$$f_{\rm C\,II}(\Upsilon) = f_{\rm C\,II}(300)(\Upsilon/300)^{7/4}\,, \tag{20}$$

and, for the same case, $\langle f_{\rm C\,II}\rangle = 4.62 f_{\rm C\,II}(300)$. The errors are only factors of order unity even in extreme cases. If the clouds are particularly perverse, then one may have, for example, a two-component model in which one component provides C II and H I, and the other supplies N V, C IV, and Si IV. Our results for $\Upsilon$ can be rendered as meaningless as desired by postulating sufficiently disparate clouds in the two-cloud model.

Regarding point (2), we can say that the cloud optical depth due to H I ionization is $\tau_\nu = 0.63[N({\rm H\ I})/10^{17}\ {\rm cm}^{-3}](\nu_c/\nu)^3$, and so $N({\rm H\ I}) > 2 \times 10^{17}\ {\rm cm}^{-2}$ will count as an optically thick cloud. Such column densities are technically possible with the range quoted in Table 5. As discussed in § IV, they are highly unlikely given the observed structure of the Ly$\alpha$ absorption line, and it is probable that the clouds are indeed optically thin.

Point (3) is supported by the work of Green *et al.* (1980) which shows that the QSOs observed with the *IUE* emit strongly to photon energies of up to 30 eV. The work by Wilson, Carnochan, and Gondhalekar (1979) observed a QSO to 38 eV. It has not yet been verified that Q0119−046, in particular, emits to these energies or that any QSO emits from 38 eV to 100 eV. They probably do, however, unless a shielding gas cloud intervenes. In Q0119−046, the clouds associated with the $z_{\rm abs} = 1.97$ complex are unlikely candidates for such shields since only perverse configurations can yield column densities $N({\rm H\ I}) > 2 \times 10^{17}\ {\rm cm}^{-2}$. There is also the $z_{\rm abs} = 1.7403$ system whose Ly$\alpha$ has a rest equivalent width $W = 1.11$ Å. It is probably blended, but, if not, it demands $n$(H I) $< 10^{18}\ {\rm cm}^{-2}$ for zero velocity spread of material and much less for reasonable velocity spreads. Thus, Q0119−046 has no good candidates for a shielding cloud.

The fine structure state C II* is populated by (1) collisional excitation; (2) direct infrared excitation; and (3) absorption and reradiation of ultraviolet radiation in the resonance lines.

In case (1), we find $n({\rm H}) > 100\ {\rm cm}^{-3}$ for the cloud density required to populate the C II* fine structure state. As we discuss below, cases (2) and (3) are not likely mechanisms for creating C II*, and we assume $n({\rm H}) > 100\ {\rm cm}^{-3}$.

It is clear from inspection of the line depths that the cloud responsible for shielding must cover much, or all, of the QSO continuum and emission line regions. In that case, it would seem safe to demand that the cloud diameter $D > 10^{18}$ cm. The column density is then

$$N({\rm H}) = n({\rm H})D > 10^{20}\ {\rm cm}^{-2} \tag{21}$$

for reasonable cloud geometries. Unless the clouds are very thin shells or filaments seen at the appropriate angle, the geometrical factor applied to correct equation (21) is of order unity. It may be argued that a thin shell ejected by the QSO may invalidate equation (21) by providing a large geometrical correction factor. However, one thing we know about the $z_{\rm abs} = 1.9644$ cloud is that it is not ejected from the QSO; rather it is falling in at 2800 km s$^{-1}$!

The ionization-structure argument for the $z_{\rm abs} = 1.9644$ cloud yielded an estimate $N({\rm H}) = 4 \times 10^{19}\ {\rm cm}^{-2}$ which is mildly inconsistent with equation (21). Two inferences can be made:

1. We need to have $D = 10^{18}$ cm and $n({\rm H}) = 100\ {\rm cm}^{-3}$ for the cloud to be as consistent as possible with our observations.

2. One of the assumptions needs some modification to achieve consistency. We feel that either the cloud geometry or the homogeneity assumption must be the most questionable one. The discrepancy is not serious, however, and we shall continue with the assumptions intact. Since $\Upsilon = 300$ and $n({\rm H}) = 100\ {\rm cm}^{-3}$, we must have a photon density $n_\gamma = 0.33$ to photoionize the gas to the required degree. If the QSO is responsible for the ionizing radiation, we must estimate the luminosity of Q0119−046 at the Lyman limit (912 Å in the QSO rest frame). If $\nu_c$ is the Lyman limit frequency, $L_{\nu_c}$ the QSO luminosity per Hz at that point, and $f_{\nu_c}$ the received flux, then

$$L_{\nu_c} = f_{\nu_c}(1+z)4\pi\left(\frac{c}{H_0}\right)^2 z^2\left(1+\frac{z}{2}\right)^2(1+z)^{-1} \tag{22}$$

or

$$L_{\nu_c} = 4 \times 10^{31}\left(\frac{60}{H_0}\right)^2\ \ ({\rm ergs\ s^{-1}\ Hz^{-1}}) \tag{23}$$

which has been computed for a universe with $q_0 = 0$. For $q_0 = 1$, we omit the factor $[1 + (z/2)]^2$, and the luminosity is less by a factor 3.9.

The ionizing photon density near a QSO is (Sargent *et al.* 1979)

$$n_\gamma = 3 \times 10^{-4}(1\ {\rm Mpc}/\Delta)^2(L_{\nu_c}/10^{31})\ \ ({\rm cm}^{-3})\,, \tag{24}$$

and we obtain

$$\Delta = 60\ {\rm kpc}\ \ (q_0 = 0)\,,\quad \Delta = 30\ {\rm kpc}\ \ (q_0 = 1)\,, \tag{25}$$

for the distance of this particular cloud from the QSO.

The limits on the size of the cloud suggest that it may only barely cover the QSO emission line region and,

indeed, may not quite do so. This introduces additional uncertainties into the line profile fits of § IV which cannot be resolved unambiguously with our data.

If some of the absorbing clouds are as close as 60 kpc to the QSO, then they may be detectable by the methods described by Sargent and Boroson (1979). The clouds will scatter photons in the resonance lines of their ion species and an extended halo of emission line luminosity will surround the QSO. The absorption lines from the cloud covering the QSO itself need not then be centrally black.

Now, we consider the possibility that collisions are not the mechanism for populating C II*. The work of Bahcall and Wolf (1968) and Sarazin, Flannery, and Rybicki (1979) is relevant to this problem. The results of those authors require gas clouds from 10 pc to 1 kpc from the QSO in order that its infrared or ultraviolet radiation be capable of populating C II*. At 1 kpc, $n_\gamma = 1.2 \times 10^3$ and $\Upsilon = 300$ would demand $n(\mathrm{H}) = 4 \times 10^5$ cm$^{-3}$. In that case, collisional excitation would be the C II* populating case anyway. Thus the demand $n(\mathrm{H}) > 100$ cm$^{-3}$ is probably secure.

### b) *Properties of the Q1115+080 Complex*

We also discuss in this paper an absorption complex with $z_{\mathrm{abs}} > z_{\mathrm{em}}$ in the gravitationally lensed object Q1115+080. The geometry of the lens effect is discussed in Young *et al.* (1981) and the absorption line data are presented in YSB. There are four systems with velocities relative to the QSO of:

$$\begin{aligned} &3{:}\ z_{\mathrm{abs}} = 1.7283\,, \quad v = -360 \text{ km s}^{-1}\,; \\ &4{:}\ z_{\mathrm{abs}} = 1.7304\,, \quad v = -580 \text{ km s}^{-1}\,; \\ &5{:}\ z_{\mathrm{abs}} = 1.7322\,, \quad v = -790 \text{ km s}^{-1}\,; \\ &6{:}\ z_{\mathrm{abs}} = 1.7353\,, \quad v = -1130 \text{ km s}^{-1}\,. \end{aligned} \tag{26}$$

The QSO redshift $z_{\mathrm{em}} = 1.725 \pm 0.002$ has an uncertainty of 220 km s$^{-1}$ which is the main error in the relative velocities of the absorption and emission lines. As in the case of the $z_{\mathrm{abs}} = 1.97$ complex in Q0119−046, they are high-ionization systems with the C IV $\lambda\lambda$1548, 1550 doublet strong. System 5 has a strong N V $\lambda\lambda$1238, 1242 doublet, and all have strong Ly$\alpha$. Lines of C II, Si II, and Si III are mostly absent; Si IV is weakly seen in system 6. An ionization parameter $\Upsilon = 100$ is suggested by the line strengths of system 5. System 6 has strong Ly$\alpha$ absorption and a weak Si IV $\lambda\lambda$1393, 1402 doublet which suggests $\Upsilon = 1000$. Systems 3 and 4 do not have enough lines to estimate $\Upsilon$ reliably, but values from 100 to 1000 are suggested by the visibility of C IV and Ly$\alpha$ and the absence of observed low-ionization species.

It is not possible to set precise density limits on the absorbing gas since no ions with excited fine structure lines are visible. However, the Ly$\alpha$ absorption does become centrally black in the stronger lines, and the usual size constraint,

$$D \gtrsim 10^{18} \quad (\mathrm{cm}) \tag{27}$$

also holds for these absorbing clouds. The ionization structure and column densities would suggest

$$N(\mathrm{H}) \approx 10^{19-20} \quad (\mathrm{cm}^{-2}) \tag{28}$$

for systems 5 and 6. The column densities in systems 3 and 4 are probably somewhat less ($10^{18}$ cm$^{-2}$) but are more difficult to estimate.

The luminosity of Q1115+080, after removing the flux augmentation due to gravitational lensing, may be estimated from the photometry in Young *et al.* (1981). We find,

$$L_{\nu_c} = 5 \times 10^{30}(60/H_0)^2 \quad (\mathrm{ergs\ s^{-1}\ Hz^{-1}})\,, \tag{29}$$

as computed with a $q_0 = 0$ cosmology.

For reasonably shaped clouds,

$$n(\mathrm{H}) = N(\mathrm{H})/D \lesssim 30 \quad (\mathrm{cm}^{-3}) \tag{30}$$

for the column densities given in equation (28) and size constraint given in equation (27). The observed ionization parameter $\Upsilon = 100$–1000 then demands a cloud distance $\Delta > 22$–70 kpc for systems 5 and 6 respectively.

## VI. ORIGIN OF THE ABSORPTION COMPLEXES

In this section, we consider several possible origins for the absorption complexes with $z_{\mathrm{abs}} > z_{\mathrm{em}}$ in Q0119−046, Q1115+080, and in other QSOs (see WWBM). First, we note that it is very likely that all systems in a given complex are connected. Complexes with $z_{\mathrm{abs}} > z_{\mathrm{em}}$ are not common, and it would be most improbable for most QSOs to have no systems with $z_{\mathrm{abs}} > z_{\mathrm{em}}$ and for a few to have four, if such systems were unrelated.

### a) *Broad-Line Emission Region*

The main rationale for considering gas in or near the QSO broad-line emission region is that the velocities of the absorption systems are comparable to the QSO line widths. However, two objections seem to be fatal to this hypothesis:

1. Some of the systems have lines which reach to nearly zero intensity in their center. It is unlikely that clouds associated with the broad-line emission region could completely cover that region.

2. For the $z_{\mathrm{abs}} = 1.9644$ system in Q0119−046, we found $n(\mathrm{H}) \approx 100$ cm$^{-3}$ from direct and indirect arguments. At a distance of $\sim 1$ pc from the central source of ultraviolet radiation, such tenuous gas could not have the observed ionization structure. At 1 pc from Q0119−046, we find a photon density $n_\gamma = 10^9$ cm$^{-3}$ and that the absorption cloud density required would be $n(\mathrm{H}) = 10^{11}$ cm$^{-3}$.

### b) *Sharp Emission Line Region*

Gas clouds in the sharp emission line regions of Seyfert galaxies may extend to $\sim 1$ kpc from the galaxy nucleus. Although the velocities are usually $< 1000$ km s$^{-1}$, rare cases can have line wings up to 2500 km s$^{-1}$.

The distance limits derived in §§ V*a* and V*b* would make this uncomfortably close to the QSO, i.e., the gas density has to be $n(\mathrm{H}) \sim 10^{4-5}$ cm$^{-3}$ in order to have the

desired photoionization parameter $\Upsilon$, and this is considerably denser than the limits derived. Further, it is difficult to imagine that the gas would be falling into the QSO at speeds of up to 3500 km s$^{-1}$; ejection at that velocity would be a far more plausible explanation of high velocities in "sharp" emission line region gas. (See, however, the note in § V*a*, on these large infall velocities.)

Consequently, we feel uncomfortable with this idea of the origin of the absorption complexes.

### c) *The QSO Galaxy*

Can gas clouds in the disk halo of the putative galaxy harboring the QSO be responsible for the absorption systems? Gas in the disk of a spiral galaxy can be more or less shielded from the ultraviolet radiation of the QSO, and so the distance limits given in §§ V*a* and V*b* need not apply strictly. However, disk gas in our Galaxy does not have the high ionization structure of the observed absorption complexes, as adjudged by interstellar lines (see, for example, Morton 1978). Gas from the galaxy halo is a more realistic possibility and, indeed, one may see occasional absorption with this origin. We feel that the complexes observed do not generally arise from this source for the following reasons:

1. The velocity spread in the complexes (770 km s$^{-1}$ in Q1115+080 and 1190 km s$^{-1}$ in Q0119−046) is too large to arise from velocity spreads within a single galaxy (up to 400 km s$^{-1}$).
2. The infall velocities of up to 3870 km s$^{-1}$ are too large for motion within the QSO galaxy. (See, however, the note in § V*a* on the infall velocities.)

### d) *Surrounding Cluster of Galaxies*

WWBM discussed the possibility that the QSO was embedded in a cluster of galaxies which could provide one or more absorbing clouds correlated with the QSO redshift. It should be noted that at redshifts $z \approx 2$, when the universe was only one-third of its current age, the galaxy clusters would still be collapsing and "virializing." This has two consequences:

1. While contemporary galaxies in rich clusters are bereft of gas, they need not be at $z \approx 2$, particularly if "stripping" mechanisms are responsible.
2. A collapsing structure would preferentially yield redshifts $z_{abs} > z_{em}$ since the QSO would have to be on the far side of the cluster, falling in, to have maximum probability of intersecting clouds.

The line-of-sight velocity dispersions of rich clusters lie in the range $\sigma_v = 600$–$1500$ km s$^{-1}$ at the present epoch. Thus, the velocity spread seen in our two absorption complexes is well within this range. The mean velocity of the QSO relative to the complex is 715 km s$^{-1}$ in Q1115+080 and 3280 km s$^{-1}$ in Q0119−046. The former velocity is quite reasonable for the velocity of the QSO relative to the cluster, but, for Q0119−046, the value is uncomfortably high. It is not impossible, however, for the rare combination of a very rich structure and a 2 $\sigma$ velocity for the QSO. This explanation will fail if absorption complexes with the velocities seen in Q0119−046 are common. The work of WWBM suggests that they are not. (See, however, the note in § V*a* on the infall velocities.)

The metagalactic ultraviolet radiation field from QSOs has a photon density $n_\gamma \approx 10^{-5}$ cm$^{-3}$ ($H_0 = 60$, $q_0 = 0$) at redshifts $z \approx 2$. The light from Q0119−046 surpasses this for distances $\Delta < 11$ Mpc, and the light from Q1115+80 similarly does so for $\Delta < 4$ Mpc. If then, galaxies correlated with the QSO have clouds similar to field galaxies (which are assumed to have photoionized by the metagalactic ultraviolet radiation), then the absorption due to correlated galaxies will have ionization parameters

$$T_{corr}/T_{field} = 30(1\ \mathrm{Mpc}/\Delta)^2(L_{\nu_c}/10^{31}), \qquad (31)$$

and, for $\Delta \approx 500$ kpc and $L_{\nu_c} \approx 10^{31}$, will have ionization parameters $\sim 100$ times larger than field galaxies. Comparison of putative field galaxy systems (Sargent *et al.* 1979) with the complexes shows this to be the case.

The $z_{abs} = 1.9644$ system in Q0119−046, with C II fine structure is a special case, although systems with $z_{abs} \ll z_{em}$ may also show such lines upon occasion (Young *et al.* 1979). The system in Q0119−046 may simply be a redshift system similar to those with $z_{abs} \ll z_{em}$ except with a lower ionization parameter due to the proximity of the QSO. One may feel uncomfortable with the idea of requiring a relative cloud–QSO velocity of 2780 km s$^{-1}$ and a separation of only 60 kpc (see § V*a*), but we offer the example of the high-velocity filaments of NGC 1275 (Kent and Sargent 1979) in which $n(\mathrm{H}) =$ 10–100 cm$^{-3}$ and the relative velocity is 2900 km s$^{-1}$. It may be that the absorption line complexes are analogous to the NGC 1275 high-velocity filaments.

## VII. SUMMARY

High-resolution spectroscopic observations of the object Q0119−046 have shown the following:

1. The emission redshift is $z_{em} = 1.937 \pm 0.002$.
2. The spectrum is riddled with absorption lines, and we present a list of 61 lines in Table 3.
3. These absorption lines identify seven main redshift systems as listed in Table 4. Some of these systems have multiple components, particularly the members of a complex of absorption systems with $z_{abs} = 1.97$ (the velocities relative to the QSO range from −2780 to −3870 km s$^{-1}$).
4. The redshift systems in the $z_{abs} = 1.97$ complex have high-ionization species C IV, Si IV, and N V and photoionization parameters $\Upsilon = 100$–$300$.
5. One of the redshift systems of the "infalling" complex shows a weak C II $\lambda$1334 line and also C II* $\lambda$1335 excited fine structure. This requires a density $n(\mathrm{H}) \geq 100$ cm$^{-3}$ in the absorbing cloud. Indirect arguments suggest that this cloud is 60 kpc from the QSO and has $n(\mathrm{H}) \approx 100$ cm$^{-3}$.

We discuss the nature of the absorption complexes in Q0119−046 and Q1115+080 (see YSB). We feel that

they probably arise from a cluster of galaxies or clouds surrounding the QSO, which photoionizes the gas to yield the observed highly ionized species. The complexes may have $z_{abs} > z_{em}$ preferentially if the galaxy cluster is still collapsing. The velocity spread in the absorption complexes is reasonable for a rich cluster, but the velocity difference $z_{abs} - z_{em}$ is uncomfortably large in Q0119−046. The high-velocity filaments in the NGC 1275 system may be an example of the type of clouds that can account for such infall velocities.

We are indebted to J. B. Oke for finishing the construction of the Palomar Double Spectrograph in time for our observing run. We thank J. Fordham, K. Shortridge, and D. Walker for assistance with the IPCS. W. L. W. S. was supported by grant AST 78-23795 from the National Science Foundation, and P. Y. was supported by grant AST 80-03398. The work of A. B. and the development of the IPCS detector which made these observations possible were supported by the U.K. Science Research Council.

## REFERENCES

Bahcall, J. N., and Wolf, R. A. 1968, *Ap. J.*, **152**, 701.
Boksenberg, A., Carswell, R. F., and Sargent, W. L. W. 1979, *Ap. J.*, **227**, 370.
Green, R. F., Pier, J. R., Schmidt, M., Estabrook, F. B., Lane, A. L., and Wahlquist, H. D. 1980, *Ap. J.*, **239**, 483.
Kent, S. M., and Sargent, W. L. W. 1979, *Ap. J.*, **230**, 667.
Kinman, T. D., and Burbidge, E. M. 1967, *Ap. J. (Letters)*, **148**, L59.
McKee, C. F., Tarter, C. B., and Weisheit, J. C. 1973, *Ap. Letters*, **13**, 13.
Morton, D. C. 1978, *Ap. J.*, **222**, 863.
Sarazin, C. L., Flannery, B. P., and Rybicki, G. B. 1979, *Ap. J. (Letters)*, **227**, L113.
Sargent, W. L. W., and Boroson, T. A. 1979, *Ap. J.*, **228**, 712.
Sargent, W. L. W., Young, P. J., Boksenberg, A., Carswell, R. F., and Whelan, J. A. J. 1979, *Ap. J.*, **230**, 49.
Weymann, R. J., Williams, R. E., Beaver, E. A., and Miller, J. S. 1977, *Ap. J.*, **213**, 619 (WWBM).
Wills, D., and Netzer, H. 1979, *Ap. J.*, **233**, 1.
Wilson, R., Carnochan, D. J., and Gondhalekar, P. M. 1979, *Nature*, **277**, 457.
Young, P., Deverill, R. S., Gunn, J. E., Westphal, J. A., and Kristian, J. 1981, *Ap. J.*, **244**, 723.
Young, P., Sargent, W. L. W., and Boksenberg, A. 1982, *Ap. J.*, **252**, 10 (YSB).
Young, P. J., Sargent, W. L. W., Boksenberg, A., Carswell, R. F., and Whelan, J. A. J. 1979, *Ap. J.*, **229**, 891.

A. BOKSENBERG: Department of Physics and Astronomy, University College London, Gower Street, London WC1E 6BT, England

WALLACE L. W. SARGENT: Department of Astronomy 105-24, California Institute of Technology, Pasadena, CA 91125

PETER YOUNG: Deceased